AGU100 ADVANCING EARTH AND SPACE SCIENCE

Geophysical Research Letters

RESEARCH LETTER
10.1029/2018GL080819

Key Points:
- Tornadoes in the United States appear to be getting more powerful
- The upward trend is independent of occurrence time and changes to the damage scale
- Part of the trend is linked to increases in CIN and to an interaction between CAPE and shear

Correspondence to:
J. B. Elsner,
jelsner@fsu.edu

Citation:
Elsner, J. B., Fricker, T., & Schroder, Z. (2019). Increasingly powerful tornadoes in the United States. *Geophysical Research Letters*, *46*, 392–398. https://doi.org/10.1029/2018GL080819

Received 8 OCT 2018
Accepted 11 DEC 2018
Accepted article online 14 DEC 2018
Published online 3 JAN 2019

Increasingly Powerful Tornadoes in the United States

James B. Elsner[1], **Tyler Fricker**[1], **and Zoe Schroder**[1]

[1]Department of Geography, Florida State University, Tallahassee, FL, USA

Abstract Storm reports show an upward trend in the power of tornadoes. Quantifying the magnitude of the increase is difficult given diurnal and seasonal influences on tornadoes embedded within natural variations and made worse by changes in practices for rating damage. Here the authors solve this problem by fitting a statistical model to a metric of tornado power during the period 1994–2016. They find an increase of 5.5% [(4.6, 6.5%), 95% CI] per year in power controlling for the diurnal cycle, seasonality, natural climate variability, and the switch to a new damage scale. A portion of the trend is attributed to long-term changes in convective storm environments involving dynamic and thermodynamic variables and their interactions. Increasing power is occurring in environments where the effect of convective available potential energy is enhanced by increasing vertical wind shear. However, a majority of the trend is not attributable to changes in storm environments.

Plain Language Summary There is a clear upward trend in tornado power over the past few decades that amounts to 5.5% per year controlling for time of day, time of year, natural variability, and the switch to a new damage rating scale. Part of the trend can be attributed to long-term changes in convective storm environments involving dynamic and thermodynamic variables and their interactions.

1. Introduction

Tornadoes are nature's most violent storms with winds that can exceed 120 m/s. A mobile Doppler radar estimated a near-ground-level wind speed of 135 m/s in the Bridge Creek-Moore, Oklahoma tornado of 3 May 1999. How global warming will affect tornadoes remains an open question. It has been argued that because of data inadequacy and limited physical understanding of the processes that cause tornadoes it is difficult to detect trends related to climate change (Kunkel et al., 2013). However, this argument is based on studies that are at least 5 years old, focus exclusively on tornado occurrences, and use methods that lack ways to include intervening factors at multiple levels (e.g., hourly and seasonal). Here we focus on tornado power and use a hierarchical statistical model that controls for the known behavior of tornado activity.

We begin by noting that while the annual number of strong and violent tornadoes (EF2 or worse) has remained relatively consistent from year to year, the number of days with many tornadoes is on the rise (Brooks et al., 2014; Elsner et al., 2015; Tippett et al., 2014, 2016). An increase in the number of big tornado days implies a larger threat of damaging tornadoes (Elsner, Jagger, Widen, et al., 2014) with the percentage of violent tornadoes (EF4 or worse) increasing with increasing outbreak size (number of tornadoes). On days with 16 to 31 tornadoes less than 4% of the tornadoes are rated EF3 or worse while on days with more than 63 tornadoes more than 8% of the tornadoes are rated EF3 or worse (Table 1). Increased percentages of violent (EF4 and EF5) tornadoes with increasing tornado-day size occur as well. This leads us to hypothesize that tornadoes are becoming more powerful.

2. Results

Tornado power is metered by the energy dissipated near the ground (Fricker et al., 2017). On average, the longest lasting tornadoes generate the most extreme wind speeds (Brooks, 2004; Elsner, Jagger, & Elsner, 2014; Fricker & Elsner, 2015). And indeed, damage paths are getting longer. Multiplying path area, air density, and wind speed gives an estimate of the total energy dissipated by a tornado (Fricker et al., 2017; see section 4). For the set of 27,950 tornadoes during the period 1994–2016, the median power is 2.22 gigawatts (GW) with an interquartile range between 0.27 and 17 GW. Tornado power is highly correlated ($r > 0.9$) with the destructive potential index developed at the U.S. Storm Prediction Center (Fricker & Elsner, 2015) and with the number

Table 1
Tornado Statistics by Tornado-Day Size

Tornado-day size (No. Tor.)	Number of cases	Total number of tor.	% tor. rated intense (EF3+)	% tor. rated violent (EF4+)
1	1,088	1,088	0.37	0.00
2–3	1,068	2,581	0.39	0.00
4–7	874	4,521	0.82	0.09
8–15	644	6,921	1.99	0.38
16–31	295	6,466	3.34	0.57
32–63	103	4,355	5.49	1.08
>63	25	2,018	8.18	2.23

Note. Numbers are based on all tornado reports over the period 1994–2016. Data are from the Storm Prediction Center.

of casualties when people are present (Fricker et al., 2017). The Tallulah-Yazoo City-Durant tornado (Louisiana and Mississippi) of 24 April 2010 that killed 10 and injured 146 had an estimated power of 66,200 GW. Annual statistics of tornado power show clear upward trends with the median, quartiles, and 90th percentile all on the rise over the period 1994–2016 (Figure 1).

The observed increase in power might be the result of shifts in when and where tornadoes occur (Agee et al., 2016). Also, at least a portion of the rise is due to a change in the procedures to rate the damage left behind. The EF damage rating scale was revised from the original F scale (and was put into operational use in 2007) with better standards for determining what was previously subjective including additional structures and vegetation, expanded degrees of damage, and a better accounting of construction quality. Figure 2 shows tornado power grouped by the change in the EF rating scale (a), El Niño/La Niña (b), month of occurrence (c), and by time of day (d). Mean energy dissipation (power) is higher at night, during La Niña, in the cooler months, and after the implementation of the EF rating procedure.

To test our hypothesis of an upward trend in tornado power, after accounting for these known influences, we fit a hierarchical regression model to the per-tornado power using all available tornado reports over the period 1994–2016. The model has a log-normal distribution for the likelihood on the per-tornado power where a lower bound is set at 0.444 GW; a value just below the least powerful tornado in the record. Fixed effects in the model include the bivariate index for El NiñoŰSouthern Oscillation (ENSO) and a variable to mark the year when the switch to the new damage rating procedures were put in place (2007). Random effects include

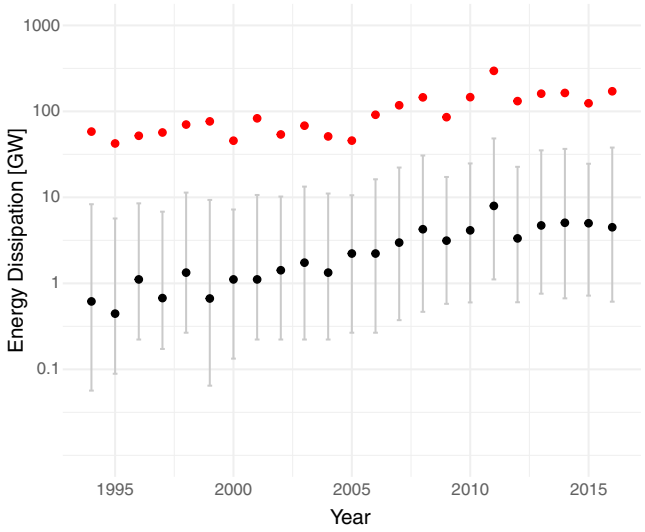

Figure 1. Annual energy dissipation (power) by year. The black dot is the median and the red dot is the 90th percentile value each year. The vertical bar extends from the lower to upper quartile numbers.

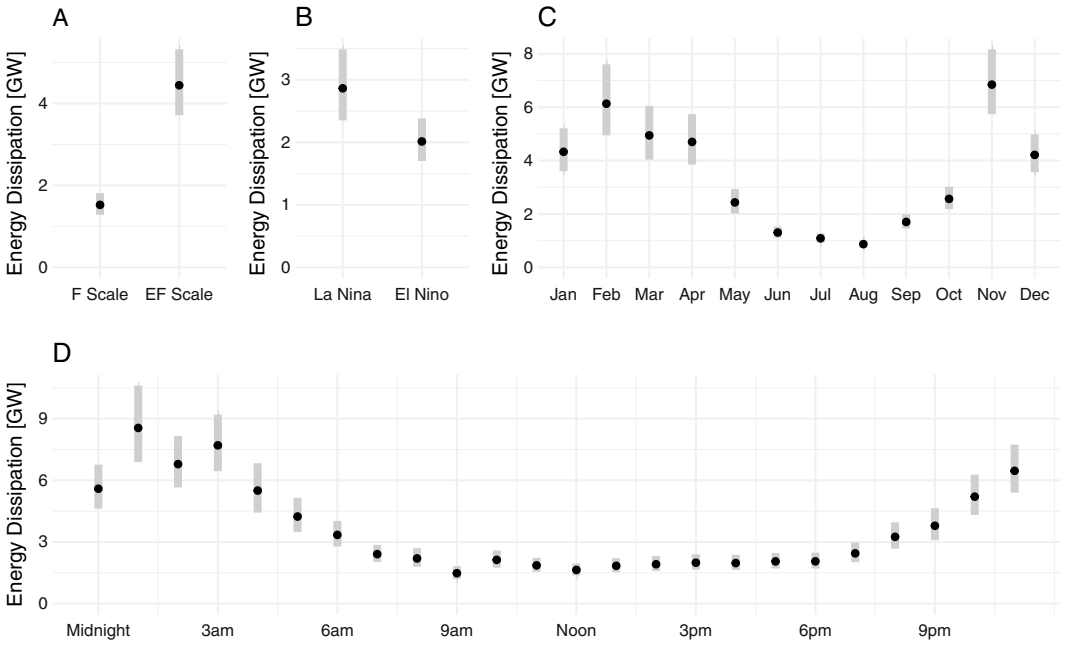

Figure 2. Energy dissipation (power) grouped by (a) EF change (b) El NiñoŰSouthern Oscillation (c) month, and (d) hour. The dot is the geometric mean for each subgroup and the gray bars extend one standard deviation from the mean.

month and hour to capture the cyclic change in energy at these respective time scales. A term indexing the year of occurrence is included as a fixed effect to test our hypothesis and to quantify the residual trend per annum (see section 4).

As expected the model shows the cycle of alternating ocean-atmosphere conditions in the equatorial Pacific, known as ENSO, is an important and significant influence on tornado power with a regression coefficient expressed as a multiplicative decrease of 0.93 [(0.90, 0.96), 95% CI] (exponentiating the coefficient in Table 2) for every one standard deviation increase (going from La Niña to El Niño) in the bivariate ENSO index. This is consistent with the fact that under La Niña conditions (especially during winter) amplified upper-air troughs move across North America. This results in warmer than normal temperatures in the Southeast and cooler than normal temperatures in the Northwest, which sets the stage for severe weather outbreaks that are intensified by a strong jetstream (Allen et al., 2015; Cook & Schaefer, 2008; Cook et al., 2017). The model also shows that the procedures put in place following the adoption of the EF damage rating scale results in an increase in power by a factor of 1.41 [(1.24, 1.59), 95% CI]. This increase is expected given the improvements after adoption in damage surveys including more precise and inclusive damage indicators.

Most importantly the model shows a significant upward trend in tornado power at a rate of 5.5% [(4.6, 6.5%), 95% CI] per year. The magnitude of the increase depends on the data and the model that controls for diurnal and seasonal variability, the ENSO cycle, and implementation of the EF rating scale. The model quantifies the increasing ferocity of tornadoes independent of the other factors considered and lends support to our

Table 2
Fixed Effects

	Estimate	Error	l-95% CI	u-95% CI
α	21.298	0.023	21.253	21.344
β_{ENSO}	−0.068	0.016	−0.101	−0.036
$\beta_{EF?}$	0.341	0.063	0.217	0.462
β_{Year}	0.054	0.005	0.045	0.063

Note. Estimated coefficients on the fixed effects terms in the model. The Error is one standard deviation. The lower and upper 95% credible intervals are given.

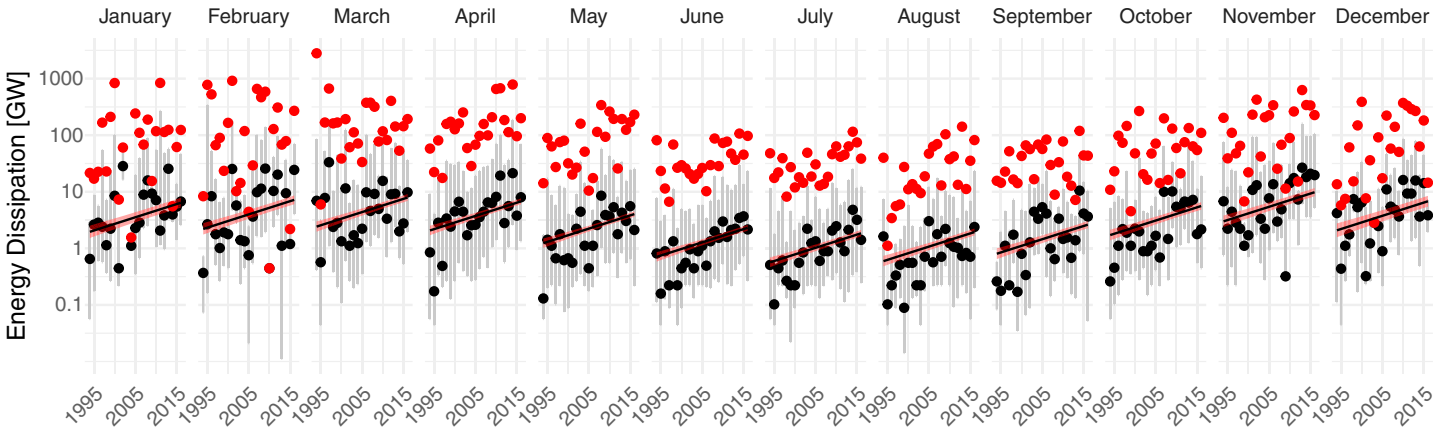

Figure 3. Upward trends in energy dissipation (power) by month. The black dot is the median and the red dot is the 90th percentile value each year. The vertical bar extends from the lower to upper quartile numbers. The black line is the modeled trend with a 95% CI band shown in red shading.

hypothesis that as tornado days become larger the tornadoes themselves are becoming more powerful. The base rate from which the upward trend depends on the time of the year through the random-effect term, but the monthly trends appear to track the data well (Figure 3).

3. Discussion

The study is retrospective but our hierarchical modeling strategy can help uncover clues about what might be happening as the Earth warms. We conjecture that at least a portion of the upward trend in tornado power is related to long-term changes in regional environments associated with severe thunderstorms. Modeling studies project increases in convective available potential energy (CAPE) with a warmer climate (DelGenio et al., 2007; Diffenbaugh et al., 2013; Trapp et al., 2009), and we previously hypothesized that climate change and increases in CAPE could be leading to more active areas of severe convection on days with tornadoes (Elsner, Jagger, & Elsner, 2014). Increases in CAPE with global warming are documented in both climate models (Sobel & Camargo, 2011) and cloud-system-resolving models (Romps, 2011), and these increases have theoretical support (Seeley & Romps, 2015; Singh & O'Gorman, 2013).

Here we examine how regional environmental factors including CAPE, convective inhibition (CIN), and storm relative helicity (SRH) are related to the trend in tornado power. We use gridded reanalysis data at 1800 UTC on big tornado days with at least 10 tornadoes (there are 748 big days in the period January 1994 through September 2014). We spatially average each of the three environmental variables separately over all grid point values within the domain defined by all the tornado genesis locations for that day. Averages over all outbreak days by year show upward trends in SRH (Tippett et al., 2016) and CIN (Figures 4b and 4c). We include the environmental variables in models for average tornado power (averaged over all tornadoes in the outbreak and divided by the area of the domain) and find the best model when CAPE and SRH are used as an interaction term (equation (3)). In other words, the model indicates that CAPE's effect on tornado power is significantly enhanced with increasing SRH (Figure 4a). For example, with average SRH values at 100 J/kg tornado power increases by 18% per 1,000 J/kg of CAPE but with average SRH values of 250 J/kg power increases by 55% for the same 1,000 J/kg of CAPE. The conditionality in the effect of CAPE on SRH is not detectable if we analyze the data without the interaction term, since in this case the model assumes that the relationship of tornado power with respect to CAPE and SRH is the same regardless of the value of the other variable. Importantly the magnitude of the trend in a model that includes the three environmental variables is 24% lower compared with the magnitude of the trend in a model that excludes them. Thus, we conclude that increasing tornado power is occurring in environments with increasing CIN and in environments where the effect of CAPE is being enhanced by increasing SRH. However, a majority of the trend is not attributable to changes in storm environments.

In summary, we identified an upward trend in tornado power (computed from the official records) after accounting for known factors and then demonstrated that a portion of the trend is statistically related to CAPE conditional on SRH. More definitive answers to important questions concerning climate change and

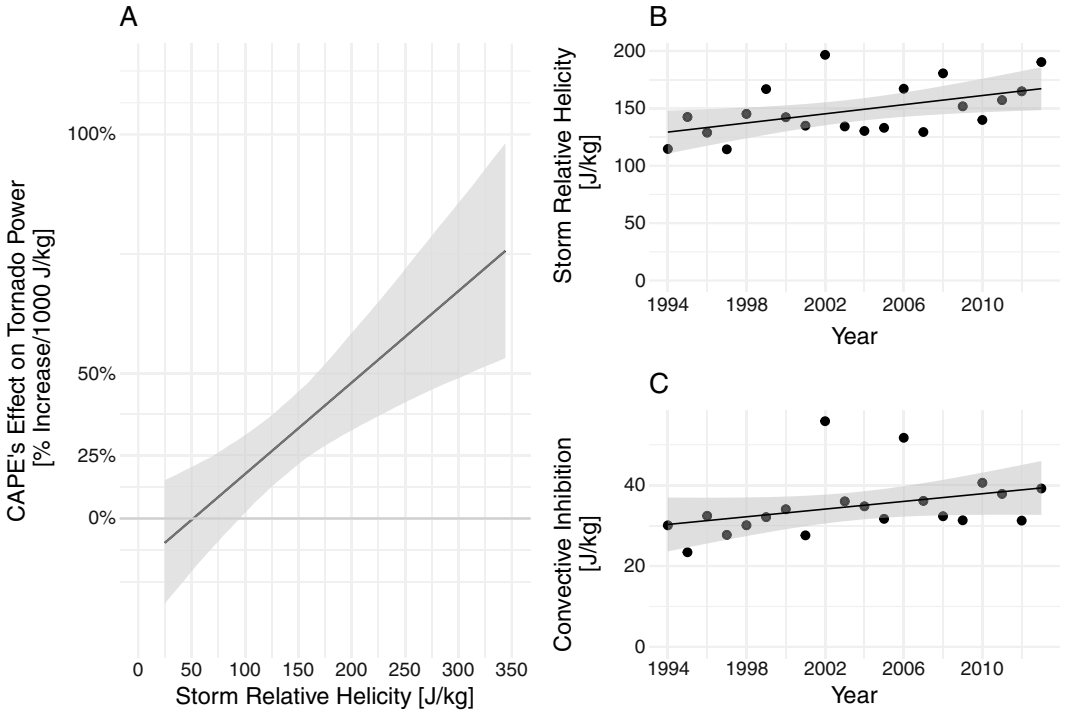

Figure 4. Upward trends in storm relative helicity, convective inhibition, and the conditional effect of CAPE. The sloping black lines denote point estimates of the trends and the gray ribbons indicate the 95% uncertainty bound around the point estimates. (a) CAPE's effect on power conditional on the value of storm relative helicity. (b) Annual values of storm relative helicity on days with at least 10 tornadoes. (c) Annual values of convective inhibition on days with at least 10 tornadoes. CAPE = convective available potential energy.

tornadoes will need to wait for a better theoretical understanding of tornado processes. But, the large number of tornadoes that occur each year provides a generous sample that allows researchers to use hierarchical models to separate potential climate change signals from noise.

4. Methods

4.1. Tornado Power (Energy Dissipation)

We calculate tornado power (P) using the energy dissipation equation defined in Fricker et al. (2017) as

$$\mathrm{P} = A_p \rho \sum_{j=0}^{5} w_j v_j^3, \tag{1}$$

where the summation is over the six possible EF ratings (0, 1, 2, 3, 4, and 5), A_p is the area of the tornado's path (units of square meters), ρ is air density (1 kg/m^3), v_j is the midpoint wind speed (m/s) for each damage rating (EF scale) j, w_j is the corresponding fraction of path area by damage rating. Multiplying the units from the individual terms results in P having units of power [kg·m^{-2} ·s^{-3} = J/s = Watt (W)]. Path area is the product of path width and path length. Path length is known to a relatively high degree of accuracy (Doswell et al., 2006). Path length and width and maximum EF rating are listed in the Storm Prediction Center's tornado database.

The database is compiled from the National Weather Service's *Storm Data* and includes all known tornadoes dating back to 1950. Here we focus on the available recent period of this record from 1994 to 2016. The start year of 1994 marks the beginning of the extensive use of the WSR-88D radar. The fraction of path area is that recommended by the U.S. Nuclear Regulatory Commission (Fricker & Elsner, 2015), which combines a Rankine vortex with empirical estimates derived from detailed storm surveys (Ramsdell & Rishel, 2007). Threshold wind speeds for the EF ratings are a 3-s gust. With no upper bound on the EF5 wind speeds, the midpoint wind speed is set at 97 m/s (7.5 m/s above the threshold wind speed consistent with the EF4 midpoint speed relative to its threshold). Tornado power is highly correlated with the destructive potential index (Fricker & Elsner, 2015; Thompson & Vescio, 1998). Additional details and justification for using tornado power are given in Fricker et al. (2017). Power by EF rating is given in Table 3.

Table 3
Tornado Power by EF Rating

(E)F Rating	*n*	Median	Total	Arithmetic mean	Geometric mean
0	17,182	0.5	73,329.6	4.3	0.6
1	7,735	12.5	364,162.5	47.1	10.8
2	2,224	91.4	609,230.8	273.9	77.5
3	650	615.7	827,474.3	1,273.0	495.4
4	145	1,631.0	511,177.8	3,525.4	1,427.6
5	14	6,458.5	130,239.0	9,302.8	5,622.7

Note. Numbers are in gigawatts (GW) and are based on the 27,950 tornadoes over the period 1994–2016.

4.2. ENSO and Environmental Variables

The ENSO variable is the bivariate ENSO (BEST) monthly series that uses a combination of the standardized Southern Oscillation Index with a standardized Niño 3.4 sea surface temperature series. We download values of the series from the Earth System Research Laboratory, Physical Science Division (NOAA/OAR/ESRL PSD). Environmental variables including CAPE, CIN, and SHR are from National Climatic Data Centers North American Regional Reanalysis (NARR) data set, which is also available from ESRL PSD. Each NARR file is available as a 277 by 349 rectangular raster that encompasses the entire United States. We download the 18 UTC data for each big day because tornado activity generally peaks in the early afternoon. The available NARR data set ends after September 2014 so we use only the big days that occur between January 1994 and September 2014.

4.3. Statistical Models

For each tornado a log-normal distribution is assumed for power with a lower bound set to 0.444 GW. The geometric means of the distributions are logically related to the fixed effects and their coefficients (β's) including year of occurrence, the bivariate ENSO index, and an indicator variable to mark the year when the switch to the new damage rating procedures were put in place (2007). Variations in power by month and hour are modeled as random intercept effects so the corresponding coefficients are vectors of length 12 and 24, respectively. Mathematically the regression model is

$$\begin{aligned}\ln(\mathrm{P}|\mathrm{P}>444000) = \alpha + \beta_{\mathrm{Year}}\mathrm{Year} + \beta_{\mathrm{ENSO}}\mathrm{ENSO} + \beta_{\mathrm{EF?}}\mathrm{EF?} + \boldsymbol{\beta}_{\mathrm{Month}}(1|\mathrm{Month}) + \\ + \boldsymbol{\beta}_{\mathrm{Hour}}(1|\mathrm{Hour}).\end{aligned} \tag{2}$$

To examine the influence environmental variables including CAPE, CIN, and SRH have on reducing the upward trend, a similar regression model is fit to power per unit area (p = P/A) averaged over all tornadoes on a day with at least 10 tornadoes. A model using outbreak-level data (rather than tornado-level data) is needed because the scale of individual tornadoes is much smaller than the scale at which the environmental variables are resolved. Here values for the environmental variables on a regular grid are the average over a convex polygon domain enclosing all the tornado genesis locations for that day. The best model (lowest Akaike information criterion value) includes the number of tornadoes, CIN, and an interaction between CAPE and SRH. Mathematically the regression model is

$$\begin{aligned}\ln(\mathrm{p}) = \alpha + \beta_{\mathrm{Year}}\mathrm{Year} + \beta_{\mathrm{long}}\mathrm{long} + \beta_{\mathrm{EF?}}\mathrm{EF?} + \boldsymbol{\beta}_{\mathrm{Month}}(1|\mathrm{Month}) \\ + \beta_N N + \beta_{\mathrm{CIN}}\mathrm{CIN} + \beta_{\mathrm{CAPE:SRH}}\mathrm{CAPE:SRH},\end{aligned} \tag{3}$$

where long is the centroid location of the outbreak along a line of longitude (this variable takes the place of ENSO which tends to shift tornado activity eastward during La Niña), N is the number of tornadoes in the outbreak, and CAPE:SRH indicates the interaction term between CAPE and SRH.

4.4. Code and Data Archive

Analysis and modeling are performed using the software environment R (http://www.r-project.org). Models are fit using maximum likelihood procedures with functions in the **lme4** package (Bates et al., 2015) and using Bayesian simulations in the Stan computational framework (http://mc-stan.org/) accessed through the **brms**

package (Bürkner, 2017). When using Bayesian simulations we specified mildly informative conservative priors to improve convergence and guard against overfittings. The codes and data to reproduce the results from this study are available at https://github.com/jelsner/tor-pwr-up and at https://github.com/jelsner/get_NARR. The NARR and ENSO data are provided by the NOAA/OAR/ESRL PSD, Boulder, Colorado, United States, at https://www.esrl.noaa.gov/psd/.

Acknowledgments
The code and data to reproduce the results from this study are available from https://github.com/jelsner/tor-pwr-up and https://github.com/jelsner/get_NARR.

References

Agee, E., Larson, J., Childs, S., & Marmo, A. (2016). Spatial redistribution of USA tornado activity between 1954 and 2013. *Journal of Applied Meteorology and Climatology*, *55*, 1681–1697.

Allen, J. T., Tippett, M. K., & Sobel, A. H. (2015). Influence of the El Niño/Southern Oscillation on tornado and hail frequency in the United States. *Nature Geosciences*, *8*, 278–283.

Bates, D., Mächler, M., Bolker, B., & Walker, S. (2015). Fitting linear mixed-effects models using lme4. *Journal of Statistical Software*, *67*(1), 1–48. https://doi.org/10.18637/jss.v067.i01

Brooks, H. E. (2004). On the relationship of tornado path length and width to intensity. *Weather and Forecasting*, *19*, 310–319.

Brooks, H. E., Carbin, G. W., & Marsh, P. T. (2014). Increased variability of tornado occurrence in the united states. *Science*, *346*(6207), 349–352. https://doi.org/10.1126/science.1257460

Bürkner, P.-C. (2017). brms: An R package for Bayesian multilevel models using Stan. *Journal of Statistical Software*, *80*(1), 1–28. https://doi.org/10.18637/jss.v080.i01

Cook, A. R., Leslie, L. M., Parsons, D. B., & Schaefer, J. T. (2017). The impact of El Niño-Southern Oscillation (ENSO) on winter and early spring U.S. tornado outbreaks. *Journal of Applied Meteorology and Climatology*, *56*(9), 2455–2478. https://doi.org/10.1175/jamc-d-16-0249.1

Cook, A. R., & Schaefer, J. T. (2008). The relation of El Niño-Southern Oscillation (ENSO) to winter tornado outbreaks. *Monthly Weather Review*, *136*, 3121–3137.

DelGenio, A. D., Yao, M.-S., & Jonas, J. (2007). Will moist convection be stronger in a warmer climate? *Geophysical Research Letters*, *34*, L16703. https://doi.org/10.1029/2007gl030525

Diffenbaugh, N. S., Scherer, M., & Trapp, R. J. (2013). Robust increases in severe thunderstorm environments in response to greenhouse forcing. *Proceedings of the National Academy of Sciences*, *110*, 16,361–16,366. https://doi.org/10.1073/pnas.1307758110

Doswell, C. A., Edwards, R., Thompson, R. L., Hart, J. A., & Crosbie, K. C. (2006). A simple and flexible method for ranking severe weather events. *Weather and Forecasting*, *21*(6), 939–951. https://doi.org/10.1175/waf959.1

Elsner, J. B., Elsner, S. C., & Jagger, T. H. (2015). The increasing efficiency of tornado days in the United States. *Climate Dynamics*, *45*(3-4), 651–659.

Elsner, J. B., Jagger, T. H., & Elsner, I. J. (2014). Tornado intensity estimated from damage path dimensions. *PLoS One*, *9*(9), E107571.

Elsner, J. B., Jagger, T. H., Widen, H. M., & Chavas, D. R. (2014). Daily tornado frequency distributions in the United States. *Environmental Research Letters*, *9*(2), 024018.

Fricker, T., & Elsner, J. B. (2015). Kinetic energy of tornadoes in the United States. *PLoS One*, *10*, E0131090. https://doi.org/10.1371/journal.pone.0131090

Fricker, T., Elsner, J. B., & Jagger, T. H. (2017). Population and energy elasticity of tornado casualties. *Geophysical Research Letters*, *44*, 3941–3949. https://doi.org/10.1002/2017GL073093

Kunkel, K. E., Karl, T. R., Brooks, H., Kossin, J., Lawrimore, J. H., Arndt, D., et al. (2013). Monitoring and understanding trends in extreme storms: State of knowledge. *Bulletin of the American Meteorological Society*, *94*(4), 499–514. https://doi.org/10.1175/bams-d-11-00262.1

Ramsdell, J. V. Jr., & Rishel, J. P. (2007). Tornado climatology of the contiguous United States (Tech. Rep. Nos. NUREG/CR-4461, PNNL-15112). Richland, WA: Pacific Northwest National Laboratory.

Romps, D. M. (2011). Response of tropical precipitation to global warming. *Journal of the Atmospheric Sciences*, *68*(1), 123–138. https://doi.org/10.1175/2010jas3542.1

Seeley, J. T., & Romps, D. M. (2015). Why does tropical convective available potential energy (CAPE) increase with warming? *Geophysical Research Letters*, *42*, 10,429–10,437. https://doi.org/10.1002/2015GL066199

Singh, M. S., & O'Gorman, P. A. (2013). Influence of entrainment on the thermal stratification in simulations of radiative-convective equilibrium. *Geophysical Research Letters*, *40*, 4398–4403. https://doi.org/10.1002/grl.50796

Sobel, A. H., & Camargo, S. J. (2011). Projected future seasonal changes in tropical summer climate. *Journal of Climate*, *24*(2), 473–487. https://doi.org/10.1175/2010jcli3748.1

Thompson, R., & Vescio, M. (1998). The destruction potential index—A method for comparing tornado days. In *19th Conference on Severe Local Storms* (pp. 1–5). Norman, OK.

Tippett, M. K., Lepore, C., & Cohen, J. E. (2016). More tornadoes in the most extreme U.S. tornado outbreaks. *Science*, *354*(6318), 1419–1423. https://doi.org/10.1126/science.aah7393

Tippett, M. K., Sobel, A. H., Camargo, S. J., & Allen, J. T. (2014). An empirical relation between U.S. tornado activity and monthly environmental parameters. *Journal of Climate*, *27*, 2983–2999.

Trapp, R. J., Diffenbaugh, N. S., & Gluhovsky, A. (2009). Transient response of severe thunderstorm forcing to elevated greenhouse gas concentrations. *Geophysical Research Letters*, *36*, L01703. https://doi.org/10.1029/2008GL036203